

Hydrodynamics of strictly propulsive waves

A. MONAVON (ORSAY)

WATER propulsion has been studied from a theoretical point of view for fifteen years. However, the author essentially interested in the total physical parameters associated to this kind of flow. A study of the details of the pressure field and local thrusts and powers which act on a thin waving plate is made. The description of simple shaped waves leads to ideas useful for a more involved analysis. As the wave number k grows, the situation becomes more intricate, because then we observe more than three forces pushing at the same time on the plate. Nevertheless, the principle of non-recoil is the same. In this case, the forces are shifted astern (like the wave) instead of being stationary as in the smallest wave number case. The influence of the flow parameters and particularly the wave number k on the resulting forces is investigated.

Napęd wodny od strony teoretycznej był badany od 15 lat. W niniejszej pracy autor był głównie zainteresowany wszystkimi parametrami fizycznymi związanymi z tego rodzaju przepływem. Przeprowadzono badania dotyczące szczegółów pola ciśnienia i lokalnych sił ciągu i mocy działających na cienką falującą płytkę. Opis fal prostego kształtu dostarczył użytecznych idei dla bardziej wnikliwej analizy. Gdy liczba falowa k rośnie, sytuacja staje się bardziej zawiła, gdyż wtedy obserwujemy więcej niż trzy siły napierające w tym samym czasie na płytkę. Niemniej jednak zasada nieoddziaływania zwrotnego jest ta sama. W tym przypadku siły oraz fala są przesunięte do tyłu. Fala przestaje być stacjonarna, jak w przypadku najmniejszej liczby falowej. Zbadano wpływ parametrów przepływu, a w szczególności liczby falowej k na siły wypadkowe.

Водный привод с теоретической стороны исследовался от 15 лет. В настоящей работе автор главным образом заинтересован всеми физическими параметрами, связанными с этого рода течением. Проведены исследования, касающиеся подробностей поля давления и локальных сил тяги и мощности, действующих на тонкую волнистую пластинку. Описание волн простой формы дало полезные идеи для более подробного анализа. Когда волновое число k растет, ситуация становится более сложной т.к. тогда наблюдаем больше чем три силы напора, в этом же самом моменте, на пластинку. Тем не менее однако принцип отсутствия обратного воздействия тот же сам. В этом случае силы и волны сдвинуты назад. Волна перестает быть стационарной как в случае наименьшего волнового числа. Исследовано влияние параметров течения, а в частности волнового числа k на результирующие силы.

1. Introduction

HIGH Reynolds number aquatic propulsion has been studied from a theoretical point of view for twenty-five years. We are interested in the two-dimensional waving plate. The theory of such a model has been given by Wu [1, 2], and SIEKMANN [3]. However, the authors were essentially interested in the total physical parameters associated to this kind of flow. Our objective is to study in detail the pressure field and local thrusts and powers generated by a non-recoiling wave.

2. Description of the model

The fluid is perfect and extends to infinity. It flows at free stream velocity U . A flexible plate of negligible thickness performs transverse waves which progress from left to right (Fig. 1).

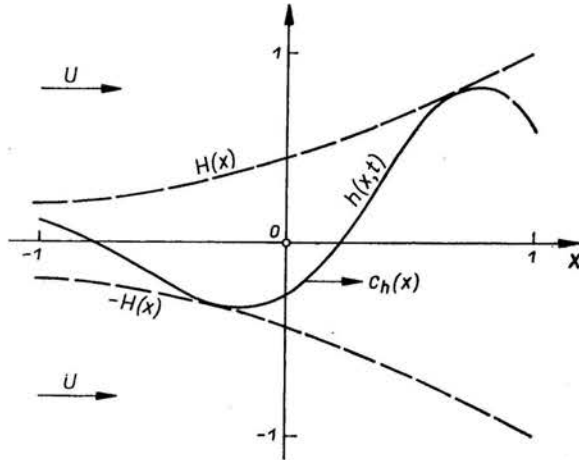


FIG. 1.

The deformation is supposed to be harmonic and described by the following equation:

$$h(x, t) = H(x)e^{j[\sigma t - kx + \epsilon(x)]}.$$

Calling ω the circular frequency, b the half-chord and k the wave-number, we have:

$$\begin{aligned} \sigma &= \omega b/U: && \text{reduced frequency,} \\ c_0 &= \sigma/k: && \text{basic phase velocity,} \\ \lambda_0 &= 2\pi/k: && \text{basic wave length.} \end{aligned}$$

The amplitude $H(x)$ remains small and so does the slope, in order to linearize the Euler equations.

The wave progresses at a phase velocity: $c_h(x) = \sigma \left(k - \frac{de}{dx} \right)$.

For the computations we have used a different formulation [1]. The wave is composed of the sum of $M+1$ basic waves which progress at the same basic phase velocity: c_0

$$h(x, t) = \left(\sum_{m=0}^M b_m e^{jem} x^m \right) e^{j(\sigma t - kx)}.$$

As a result of a selected motion, the difference between the pressure on both faces $\Delta p(x, t)$ can be computed. Pressure difference is positive when it pushes up the plate.

The forces acting on a small part of the plate are:

the lift: $dL = \Delta p dx,$

the thrust: $dT_p = -\Delta p \frac{\partial h}{\partial x} dx.$

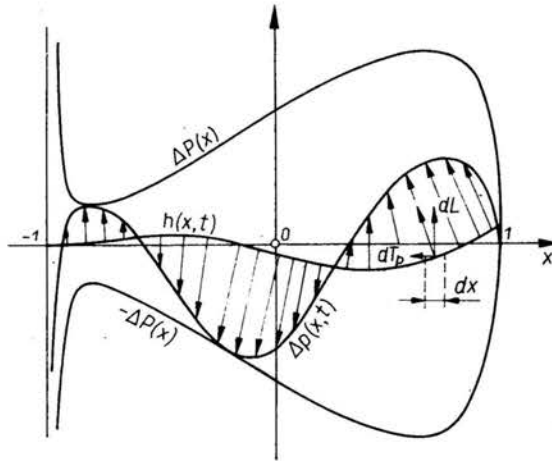


FIG. 2.

The contribution of this small segment to the total moment is: $dM = -\Delta p x dx$ and it requires a power

$$dP = -\Delta p \frac{\partial h}{\partial t} dx.$$

The distribution of both the thrust and the power are studied with their local values per unit length:

$$\mathcal{T}_p(x, t) = \frac{dT_p}{dx} / (\langle T_p \rangle / 2); \quad \mathcal{P} = \frac{dP}{dx} / (\langle P \rangle / 2)$$

which can be averaged over a time period.

After integration upon the plate we have the lift L , the moment M , the leading-edge suction T_s , the thrust T_p , and the power P . From the ratio between the total thrust and the

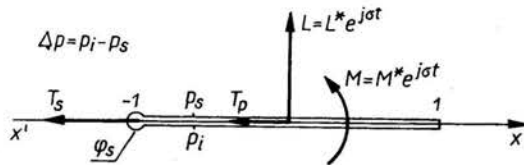


FIG. 3.

power we can define a hydrodynamic efficiency: η which measures the part of P used for propulsion, the other part being wasted into the wake.

An analytic solution of the general problem stated above has been given by WU [1]. He used the acceleration potential representation

$$\Delta p(x, t) = \left(a_0 \operatorname{tg} \frac{\theta}{2} + 2 \sum_{n=1}^{\infty} a_n \sin n\theta \right) e^{j\omega t}, \quad x = \cos \theta$$

and provided the general expressions for the a_n .

We have performed a detailed analysis of the three following fields: pressure, velocity and local forces related to simple wave shapes. Such an analysis has never been done so far. And as a continuation we have carried out the calculation of strictly propulsive waves.

3. Statement and solution of the problem

Those specific waves are calculated such as:

1) to maintain the leading-edge suction T_s at zero, in order to prevent the flow from stalling near the leading-edge;

2) to maintain both the lift and the moment at zero, in order to reduce the resulting forces acting on the plate to the sole pressure thrust T_p .

As mentioned earlier by WU [2, Part 2], the solution depends only on a finite number of basic waves. Here only four basic waves are needed to obtain strictly propulsive waves.

The two previous conditions can be stated in the following way:

$$\begin{aligned} a_0 = 0 & \Leftrightarrow T_s = 0, \\ a_0 + a_1 = 0 & \Leftrightarrow L = 0, \\ a_0 - a_2 = 0 & \Leftrightarrow M = 0, \end{aligned}$$

which reduce to $a_0 = 0$, $a_1 = 0$, $a_2 = 0$.

It can be easily shown that each a_n can be written as

$$a_n = \sum_{m=0}^M a_n^m b_m e^{j\varphi_m} \quad (n \geq 0) \quad \text{with} \quad \varphi_m = \varepsilon_m + m \frac{\pi}{2},$$

where the new coefficients a_n^m are

$$\begin{aligned} a_0^m &= a_0^{\prime m} + j a_0^{\prime\prime m} = (\mathcal{F} - 1) \lambda_1^m - \mathcal{G} \lambda_0^m + j(\mathcal{G} \lambda_1^m + \mathcal{F} \lambda_0^m); \quad \lambda_n^m = \frac{d^m}{dk^m} [(k - \sigma) J_n(k)], \\ a_n^m &= 2(-j)^{n-1} \frac{d^m}{dk^m} \left[k \left(\frac{\sigma}{k} - 1 \right)^2 J_n(k) \right] \quad (n \geq 1), \end{aligned}$$

$J_n(k)$ is the Bessel function of first kind and $\mathcal{F}(\sigma) + j\mathcal{G}(\sigma)$ the Theodorsen function [4].

If we take $b_0 = 1$ and $\varepsilon_0 = 0$, the three conditions are equivalent to a linear system of six equations

$$\begin{bmatrix} a_0^{\prime 1} & a_0^{\prime 2} & a_0^{\prime 3} & -a_0^{\prime\prime 1} & -a_0^{\prime\prime 2} & -a_0^{\prime\prime 3} \\ a_0^{\prime\prime 1} & a_0^{\prime\prime 2} & a_0^{\prime\prime 3} & a_0^{\prime 1} & a_0^{\prime 2} & a_0^{\prime 3} \\ a_1^1 & a_1^2 & a_1^3 & 0 & 0 & 0 \\ 0 & 0 & 0 & a_1^1 & a_1^2 & a_1^3 \\ a_2^1 & a_2^2 & a_2^3 & 0 & 0 & 0 \\ 0 & 0 & 0 & a_2^1 & a_2^2 & a_2^3 \end{bmatrix} \begin{bmatrix} X_1 \\ X_2 \\ X_3 \\ Y_1 \\ Y_2 \\ Y_3 \end{bmatrix} = \begin{bmatrix} -a_0^{\prime 0} X_0 + a_0^{\prime\prime 0} Y_0 \\ -a_0^{\prime\prime 0} X - a_0^{\prime 0} Y_0 \\ -a_1^0 X_0 \\ -a_1^0 Y_0 \\ -a_2^0 X_0 \\ -a_2^0 Y_0 \end{bmatrix},$$

where

$$b_m e^{j\varphi_m} = X_m + jY_m$$

and

$$X_0 = 1, \quad Y_0 = 0.$$

The coefficients of this system are functions of k and c_0 . Finally, the b_m can be divided by the same number in order to impose

$$\begin{aligned} \sup[H(x)] &= 1, \\ x &\in [-1, 1]. \end{aligned}$$

Therefore, for each value of the parameters k and c_0 we are able to compute the b_m and ϵ_m in such a way that the resulting wave satisfies the non-recoiling conditions and remains within the square $(-1 \leq x \leq 1) \times (-1 \leq y \leq 1)$.

4. Results

4.1. The wave amplitude $H(x)$

Figures 4, 5, 6 and 7 represent the variations of the amplitude $H(x)$ of the wave.

We can notice that $H(x)$ increases from the leading-edge to the trailing-edge just like the shapes that could be observed in nature. Within the range of our computations the

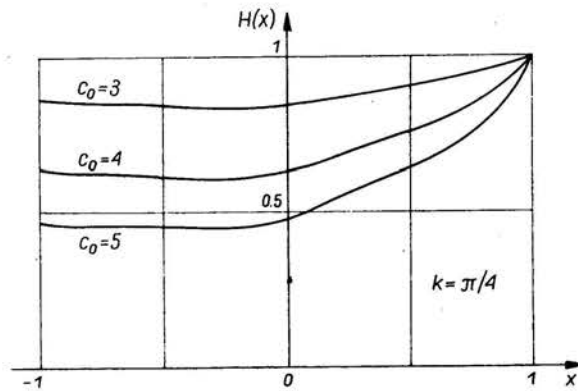


FIG. 4. $H(x)$: Amplitude of the waving-plate $h(x, t)$.

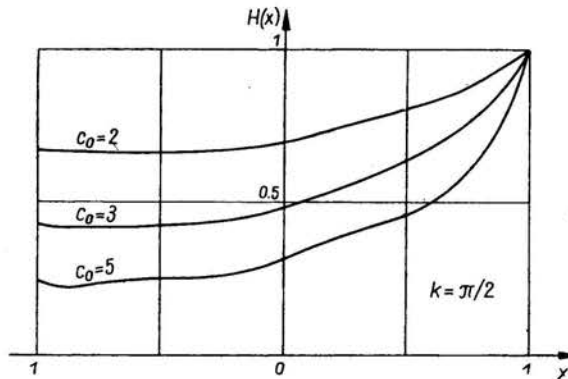


FIG. 5. $H(x)$: Amplitude of the waving-plate $h(x, t)$.

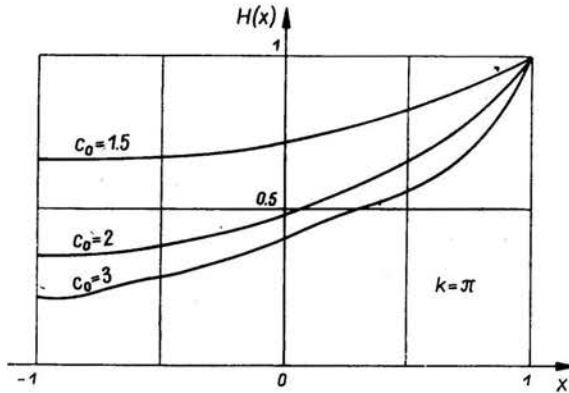


FIG. 6. $H(x)$: Amplitude of the waving-plate $h(x, t)$.

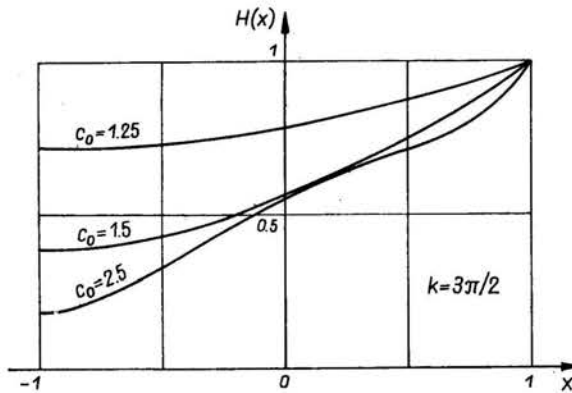


FIG. 7. $H(x)$: Amplitude of the waving-plate $h(x, t)$.

maximum of $H(x)$ remains always situated at the trailing-edge and the amplitude at the leading-edge becomes smaller as the wave-number k and the basic phase velocity c_0 become larger.

4.2. The wave phase velocity $C_h(x)$

For small wave number such as $k = \frac{\pi}{4}$ or $k = \frac{\pi}{2}$, we observe two maxima near which the wave will become "smoother" than elsewhere. As the wave number becomes larger $k = \pi$ or $k = \frac{3\pi}{2}$, these maxima disappear and then only one maximum remains.

In every case the resulting wave progresses slower than the basic waves, that is, $C_h < C_0$, whereas, near the leading-edge, the phase velocity $C_h(-1)$ remains nearly equal to one. This last remark can be explained with respect to the absence of leading-edge suction.

If we notice that a pure sinusoidal wave with constant amplitude and a phase velocity equal to one would not disturb the free stream, we can see that the leading part of the plates haws a shape similar to that quoted above.

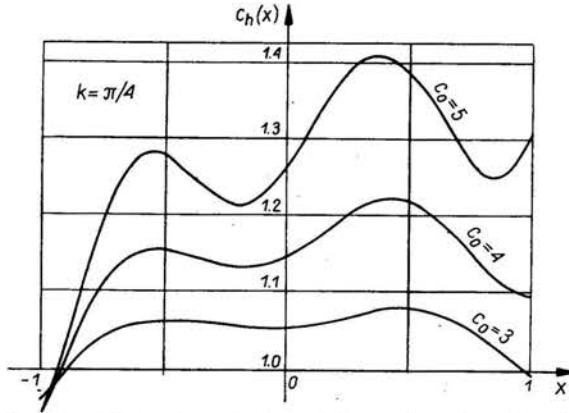


FIG. 8. $C_h(x)$: Phase velocity of the waving-plate $h(x, t)$.

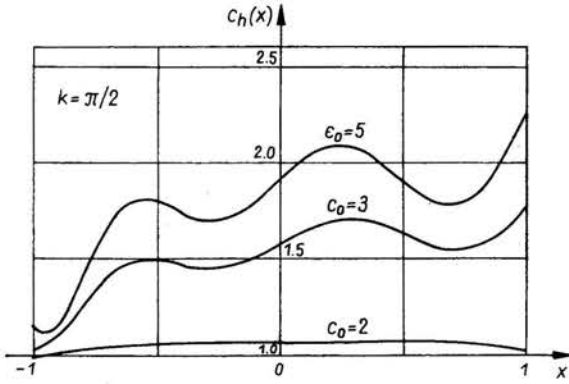


FIG. 9. $C_h(x)$: phase velocity of the waving-plate $h(x, t)$.

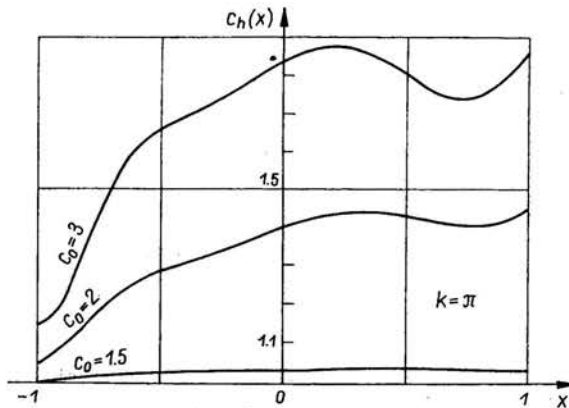


FIG. 10. $C_h(x)$: Phase velocity of the waving-plate $h(x, t)$.

Moreover, the small discrepancies from the exact value $C_h(-1) = 1$ can be inferred from the perturbations of the incident flow generated by the motions of the middle and rear parts of the plate.

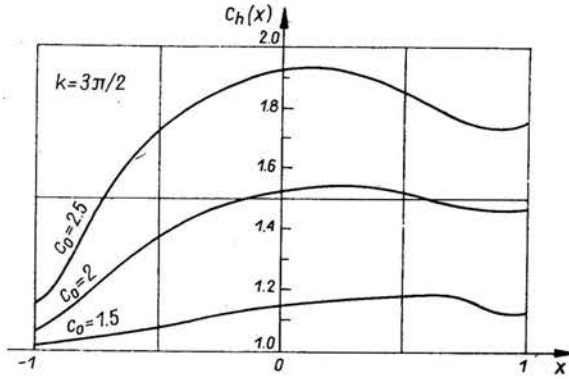


FIG. 11. $C_h(x)$: Phase velocity of the waving-plate $h(x, t)$.

4.3. Amplitude of the pressure difference $\Delta P(x)$

The wave motions described above generate a pressure difference $\Delta p(x, t)$ between both faces of the plate.

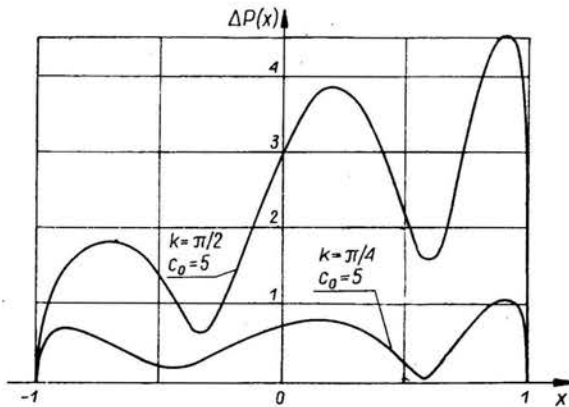


FIG. 12. $\Delta P(x)$: Amplitude of the pressure difference $\Delta p(x, t)$.

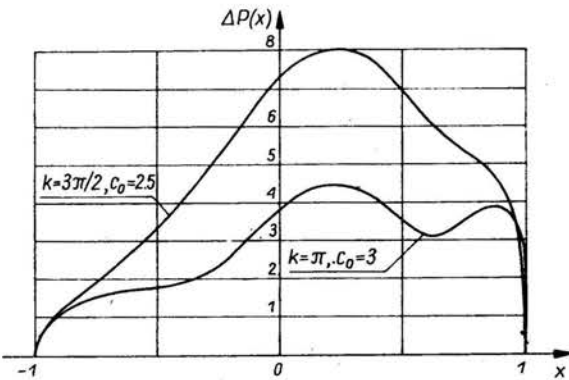


FIG. 13. $\Delta P(x)$: Amplitude of the pressure difference $\Delta p(x, t)$.

Figures 12 and 13 represent the variations of the amplitude $\Delta P(x)$ for several values of the wave number k ; we can notice that the shapes depend highly on k .

For small k , $\Delta P(x)$ shows three maxima, whereas for larger values only one maximum remains then. These features will be explained later by means of the analysis of the distributions of the lift and the moment.

In fact, the shape of $\Delta P(x)$ does not depend on C_0 . Roughly speaking, this does not appear as yet in Figs. 12 and 13; the variations of the phase velocity C_0 operate as a multiplying factor.

4.4. Phase of the pressure difference $\varphi(x)$

Associated to $\Delta P(x)$, the variations of the phase angle $\varphi(x)$ complete the description of the pressure difference Δp .

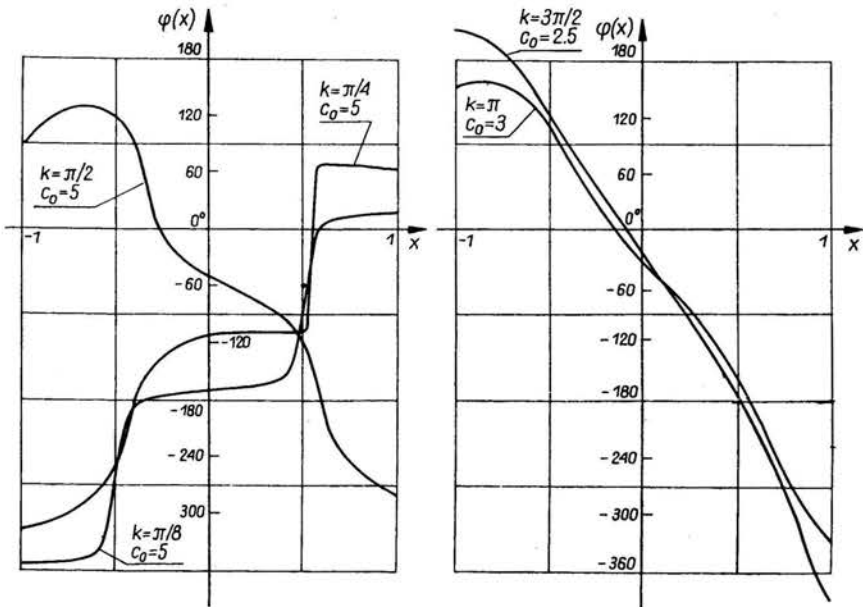


FIG. 14. $\varphi(x)$: Phase of the pressure difference $\Delta p(x, t)$.

The same shape difference can be noticed in Fig. 14. For small k , that is $k = \frac{\pi}{4}$ and $k = \frac{\pi}{8}$, $\varphi(x)$ looks like stairs. The vertical parts, where $\varphi(x)$ varies very rapidly, are located at the very same places as the amplitude minima. There is a phase angle difference of 180° between two successive steps.

For larger values of k , the variations of $\varphi(x)$ are more regular.

4.5. Phase velocity of the pressure difference $C_{\Delta p}(x)$

The same features also appear through the variations of the phase velocity of the pressure difference.

For small k , $C_{\Delta p}(x)$ varies from small values which correspond to the vertical parts of $\varphi(x)$, to very large values related to the flat steps' parts. Furthermore, it comes out that $C_{\Delta p}$ can be negative.

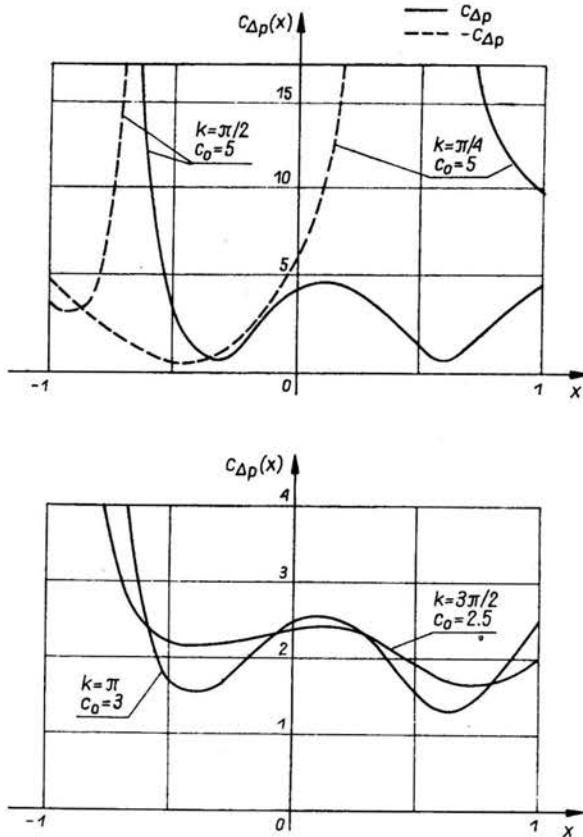


FIG. 15. $C_{\Delta p}(x)$: Phase velocity of the pressure difference $\Delta p(x, t)$.

On the contrary, when k is larger, $C_{\Delta p}$ does not vary very rapidly. This means that the pressure difference progresses with an approximately constant phase velocity far from the leading-edge.

5. Non-recoiling mechanisms

From the previous remarks we can deduce two different mechanisms which allow for zero lift and zero moment.

5.1. Case of small wave numbers

As we can see in Fig. 16 the envelope of $\Delta p(x, t)$ is constituted of three parts separated by throttles where Δp is always nearly zero.

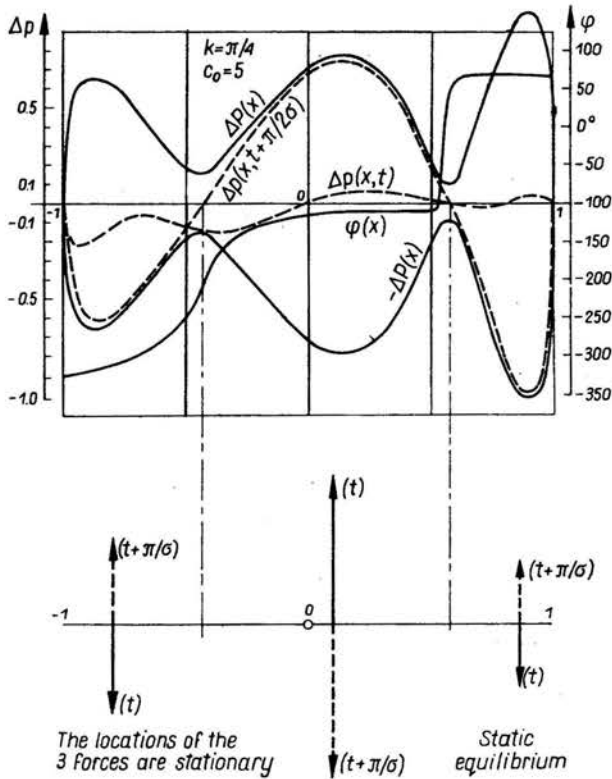


FIG. 16. Sketch of the lift and moment generation mechanism.

Within each of these parts the phase velocity $C_{\Delta p}$ is very large. Finally, the phase difference between two adjacent parts turns out to be 180° .

Therefore, we can roughly consider that $\Delta p(x, t)$ oscillates like a string and generates three distinct forces, each one corresponding to one alternation.

Yet in order to satisfy the zero lift condition, the sum of these forces has to be zero, which implies the relative magnitude of the three parts.

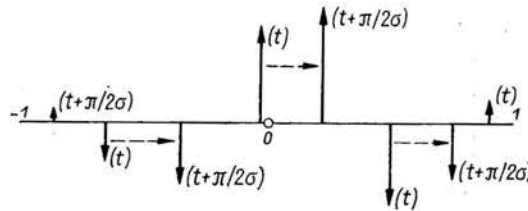
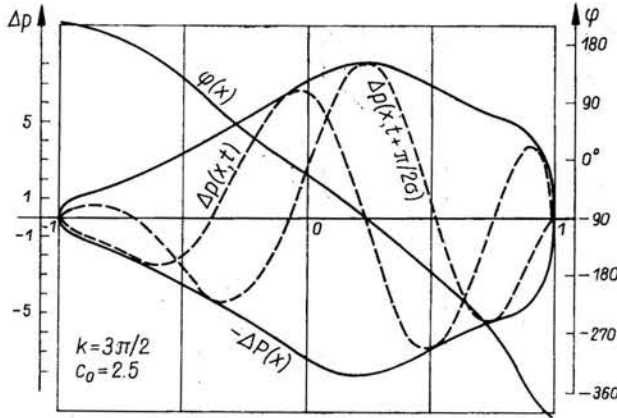
And the moment will be zero when two lateral forces push together on the central one which acts as a pivot. This requirement is satisfied by the phase difference of 180° which has been quoted earlier. Since the locations of the three forces are nearly stationary, we can speak of static equilibrium.

5.2. Case of large wave numbers

The second mechanism appears with large values of the wave number k , Fig. 17.

Now the amplitude $\Delta P(x)$ exhibits only one maximum. The phase velocity is roughly constant over the plate and slightly smaller than C_0 . Hence $\Delta p(x, t)$ progresses astern and shows three or four alternations.

The lifting effect of $\Delta p(x, t)$ can be represented as the sum of three or four forces, each one corresponding to one alternation and travelling astern at the same velocity as Δp .



Dynamic equilibrium between 3 of 4 forces which are travelling astern along the plate

FIG. 17. Sketch of the lift and moment generation mechanism.

In order to obtain zero lift and zero moment, the same conditions as stated for the first mechanism should be satisfied for every time t . But since the forces travel from the leading-edge to the trailing-edge, they realize a dynamic equilibrium.

6. Thrust generation mechanism

Since no condition is required to obtain a special distribution of the thrust, the variations of the local thrust per unit length $\mathcal{F}_p(x, t)$ do not exhibit characteristic features.

However, for a given wave number k we can notice a particular value of C_0 which leads to an almost positive distribution of \mathcal{F}_p .

When C_0 is small, for instance $C_0 = 1.25$, the pressure field and the waving plate are quite out of phase (Fig. 18).

Then, for increasing values of C_0 it appears that the phase angle difference between $\Delta p(x, t)$ and $h(x, t)$ becomes smaller.

When $C_0 = 2$, $\mathcal{F}_p(x, t)$ is positive everywhere and the phase angle difference is equal to $\pi/2$ (Fig. 19). Then, every segment of the plate generates a thrust.

When considering large values of C_0 , $\Delta p(x, t)$ is more and more shifted relatively to

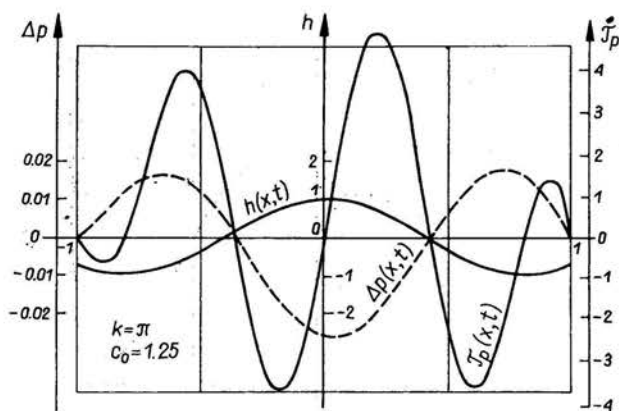


FIG. 18. Sketch of the thrust generation mechanism.

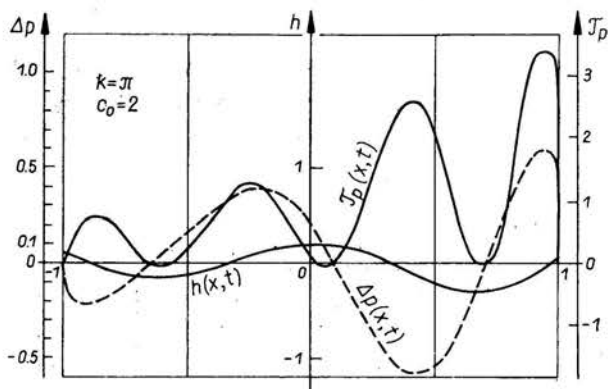


FIG. 19. Sketch of the thrust generation mechanism.

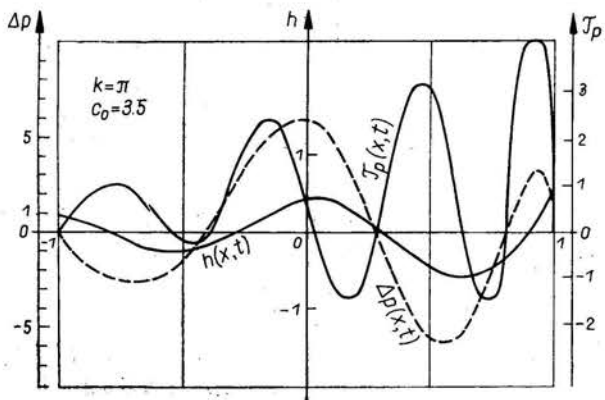


FIG. 20. Sketch of the thrust generation mechanism.

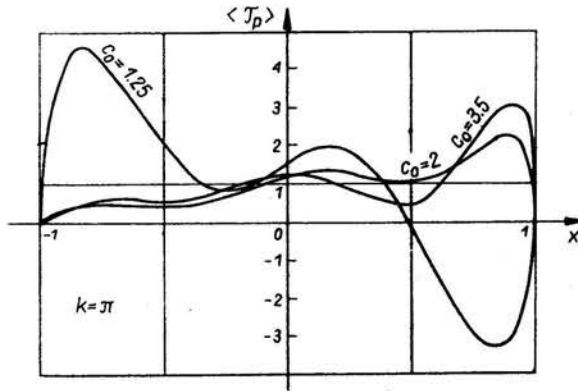


FIG. 21. Mean local thrust per unit length.

$h(x, t)$. Eventually, for $C_0 = 3.5$ they are nearly in phase together and some parts of the plate generate a drag although the total streamwise force remains a thrust.

These results are summarized in Fig. 21.

We have plotted the average value over a time period of $\mathcal{T}_p(x, t)$. Here we can see that the average distribution of the thrust upon the plate can be locally negative.

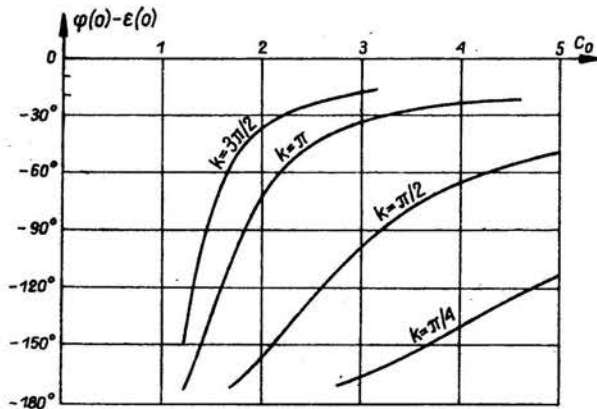


FIG. 22. Phase difference at $x = 0$ between $\Delta p(0, t)$ and $h(0, t)$.

Figure 22 shows the variations of the phase angle difference between Δp and h at the middle of the plate. This gives an approximative idea of the shift between the pressure difference and the waving plate near a maximum of $\Delta P(x)$.

For increasing values of k , the optimum value of C_0 decreases. However this particular result is of secondary importance since we know from a paper by Wu [2] that it is possible to compute waves which minimize the kinetic energy wasted into the wake under the constraint of the fixed total thrust T .

7. Hydrodynamics efficiency

Nevertheless, a very simple result that we have discovered through our computations is the expression of the hydrodynamic efficiency η .

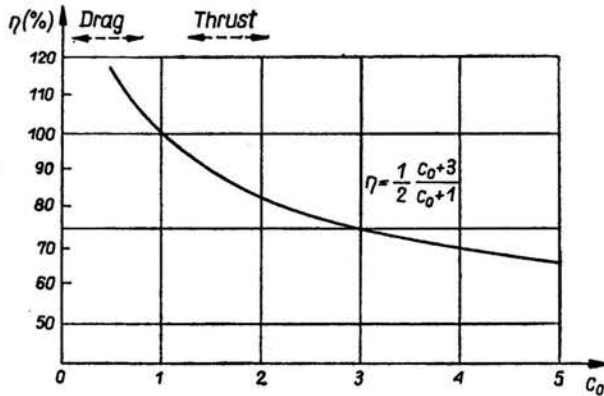


FIG. 23. η : Hydrodynamic efficiency ($\forall k$).

It appears that η only depends on the basic phase velocity C_0 and does not depend on the wave number k .

η is given by the following formula:

$$\eta = \frac{1}{2} \frac{C_0 + 3}{C_0 + 1},$$

which is valid within the range of our computations.

References

1. T. Y. WU, *J. Fluid Mech.*, 10, 321-344, 1961.
2. T. Y. WU, *J. Fluid Mech.*, 46, 337-355, 521-544, 545-568, 1971.
3. J. SIEKMANN, *Ing. Arch.*, 31, 214-228, 1962.
4. Y. LUKE, M. A. DENGLER, *J. Aero. Sci.*, 18, 478-483, 1951.

LABORATOIRE DE MÉCANIQUE EXPÉRIMENTALE DES FLUIDES,
ORSAY, FRANCE.

Received September 27, 1977.